Protein Science (1995), *4*:1528–1534. Cambridge University Press. Printed in the USA.

Structural energetics of barstar studied by differential scanning microcalorimetry

PATRICK L. WINTRODE, YURI V. GRIKO, AND PETER L. PRIVALOV
Department of Biology and Biocalorimetry Center, The Johns Hopkins University, Baltimore, Maryland 21218

(RECEIVED March 22, 1995; ACCEPTED May 22, 1995)

Abstract

The energetics of barstar denaturation have been studied by CD and scanning microcalorimetry in an extended range of pH and salt concentration. It was shown that, upon increasing temperature, barstar undergoes a transition to the denatured state that is well approximated by a two-state transition in solutions of high ionic strength. This transition is accompanied by significant heat absorption and an increase in heat capacity. The denaturational heat capacity increment at ≈75 °C was found to be 5.6 ± 0.3 kJ K^{-1} mol^{-1}. In all cases, the value of the measured enthalpy of denaturation was notably lower than those observed for other small globular proteins. In order to explain this observation, the relative contributions of hydration and the disruption of internal interactions to the total enthalpy and entropy of unfolding were calculated. The enthalpy and entropy of hydration were found to be in good agreement with those calculated for other proteins, but the enthalpy and entropy of breaking internal interactions were found to be among the lowest for all globular proteins that have been studied. Additionally, the partial specific heat capacity of barstar in the native state was found to be 0.37 ± 0.03 cal K^{-1} g^{-1}, which is higher than what is observed for most globular proteins and suggests significant flexibility in the native state. It is known from structural data that barstar undergoes a conformational change upon binding to its natural substrate barnase. Our data, which indicate that barstar has a loosely packed interior, suggest that high conformational flexibility of barstar's native structure may play an important role in allowing it to optimize its contacts with barnase upon binding without disrupting favorable, tightly packed internal interactions.

Keywords: barstar; protein stability; scanning microcalorimetry

The interaction between barnase, the extracellular ribonuclease of *Bacillus amyloliquefaciens*, and barstar, its natural inhibitor, has attracted a great deal of attention as a good model for the study of protein-protein recognition (Hartley, 1993; Schreiber & Fersht, 1993a). The crystal structure of Cys 40, 82 Ala barstar complexed with barnase was recently solved with a resolution that is sufficient for detailed analysis of the interactions stabilizing the complex (Guillet et al., 1993; Buckle et al., 1994), and the structures of both free barnase (Mauguen et al., 1982; Bycroft et al., 1991) and free barstar (Lubienski et al., 1994) are known. To understand the mechanisms by which these proteins associate with one another, we require knowledge of the thermodynamics of complex formation and the energetics of native structure formation in both free barnase and free barstar. Although the energetics of barnase have been studied in detail by several groups (Hartley, 1968, 1975; Makarov et al., 1993; Griko et al., 1994; Sanz et al., 1994), the energetics of native barstar are less well understood. The free energy of barstar unfolding by urea was estimated by Schreiber and Fersht (1993b), and the van't Hoff enthalpy of barstar unfolding was recently estimated by Agashe and Udgaonkar (1995). However, the energetics of barstar unfolding have yet to be measured in a direct, model-independent manner. In this study we have endeavored to make direct calorimetric measurements of the thermodynamic parameters associated with the disruption of Cys 40, 82 Ala barstar's native structure.

Reprint requests to: Peter L. Privalov, Department of Biology, The Johns Hopkins University, 3400 North Charles St., Baltimore, Maryland 21218; e-mail: peter@kelvin.bio.jhu.edu.

Results

Effect of pH on the thermostability barstar

Figure 1 shows the temperature dependence of the partial specific heat capacity of barstar in solutions of different pH. It is clear from the figure that the thermal denaturation of barstar is accompanied by significant absorption of heat. The temperature at which denaturation occurs depends on the pH of the solution. With increasing pH, the denaturation peaks shift to lower temperatures, showing that the protein structure becomes less stable. This change in stability is, however, quite small between pH 6.3 and 9.5 because this range is close to the isoelec-

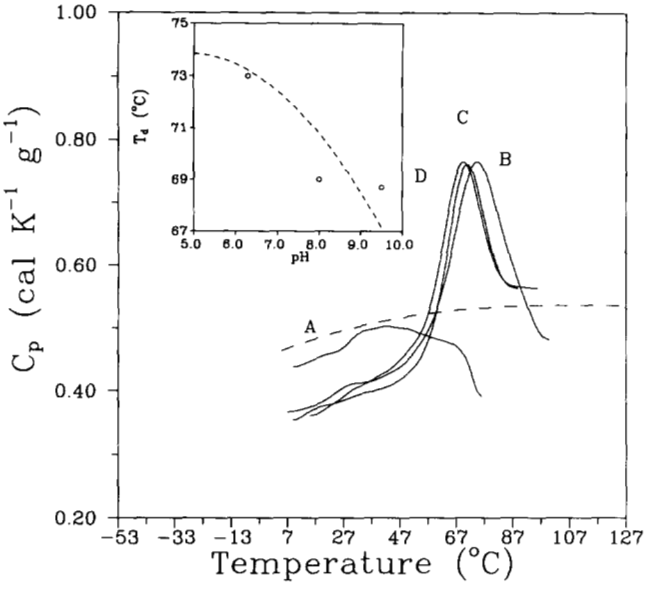

Fig. 1. Partial specific heat capacity of barstar as a function of temperature measured by DSC under different conditions of pH. A, pH 4.2. B, pH 6.3. C, pH 8.0. D, pH 9.5. The dashed line represents the heat capacity of unfolded barstar calculated assuming it to be a completely extended chain. Inset shows the expected dependence (dashed line) of the transition temperature on pH (circles represent experimental values).

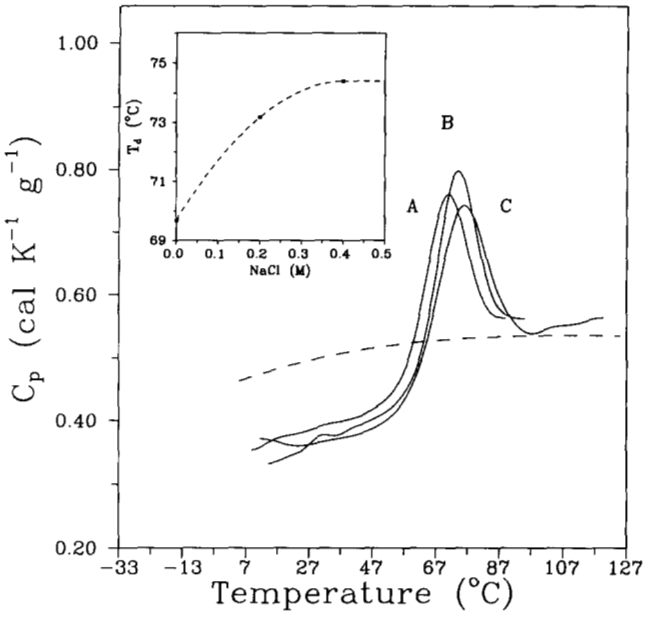

Fig. 2. Partial specific heat capacity of barstar as a function of temperature measured by DSC at pH 8.0 with different concentrations of NaCl. A, 0 mM NaCl. B, 200 mM NaCl. C, 400 mM NaCl. The dashed line is the same as in Figure 1. Inset shows the dependence of T_d on NaCl concentration.

tric point of barstar (estimated to be at pH 5.3). Decreasing the pH toward the isoelectric point leads to an increase in structural stability, which is expected to reach its maximum around pH 5.0 and drop down below this value (Fig. 1). Indeed, below this pH, the stability of barstar drops so quickly that, at pH 4.2, its pretransition heat capacity was close to that of the denatured state, and its denaturation is not accompanied by any measurable absorption of heat, indicating that it retains no stable tertiary structure (Fig. 1) (see Khurana & Udgaonkar, 1994). Upon heating at this pH, barstar was observed to aggregate above ≈67 °C.

Effect of salt on the thermodynamic parameters of barstar denaturation

Figure 2 shows the temperature dependence of the partial specific heat capacity of barstar in salt-free solution and in the presence of 200 mM and 400 mM NaCl at pH 8.00. The increase in NaCl concentration leads to an increase in the thermal stability of barstar with a corresponding increase in denaturational enthalpy. Note that, in the presence of 400 mM NaCl, the calorimetric enthalpy of barstar denaturation is very close to the van't Hoff enthalpy calculated assuming a two-state transition (Table 1).

Heat capacity

The partial specific heat capacity of native barstar is 0.38 ± 0.03 cal K^{-1} g^{-1} at 20 °C and does not appear to depend significantly on pH when the protein is in its native state. With increasing temperature, the heat capacity increases linearly with a slope of about 0.01 cal/K^2 g. It increases significantly in the range of the denaturational transition and becomes approximately 0.56 ± 0.03 cal K^{-1} g^{-1} at 95 °C, which is close in value to that calculated for the unfolded polypeptide chain of barstar at this temperature. Thus, according to the heat capacity criteria, barstar is in the unfolded conformation after heat denaturation.

Table 1. *Thermodynamic parameters associated with the thermal denaturation of barstar under different conditions of pH and salt concentration obtained from calorimetric measurements*

pH	[NaCl] (mM)	T_d (K)	ΔH_{cal} (kJ mol^{-1})	ΔH_{vH} (kJ mol^{-1})	R (cal/vH)	ΔC_p (kJ K^{-1} mol^{-1})
6.3	0	346.8	196.5 ± 10	209.5 ± 10	0.94	–
8.0	0	342.7	178.2 ± 9	250.9 ± 12	0.71	5.9 ± 0.3
9.5	0	341.7	172.4 ± 9	234.6 ± 12	0.73	5.7 ± 0.3
8.0	200	345.9	190.6 ± 9	263.0 ± 12	0.72	6.1 ± 0.3
8.0	400	347.5	211.3 ± 11	219.0 ± 11	0.96	5.7 ± 0.3

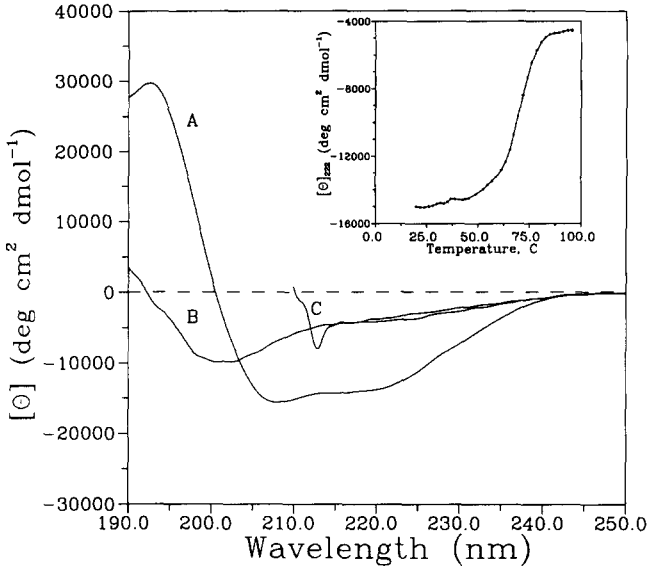

Fig. 3. Far-UV CD spectra of barstar under different conditions. A, pH 8.0, 20 °C. B, pH 8.0, 95 °C. C, pH 2.5, 6 M GuHCl, 95 °C. Inset shows the ellipticity at 222 nm as a function of temperature.

This conclusion also follows from analysis of the ellipticity of barstar at 222 nm (Fig. 3). At 95 °C, the far-UV CD spectrum of barstar in 10 mM $NaPO_4$, pH 8.0, is very similar to that of barstar in 6 M GuHCl, pH 2.5, at 95 °C, indicating that it is close to fully unfolded at this temperature. The denaturational heat capacity increment for barstar determined by extrapolation of heat capacity function for the native and denatured state to the transition temperature T_d is 5.8 ± 0.3 kJ K^{-1} mol^{-1}.

Enthalpy of heat denaturation

The experimentally measured enthalpy of barstar denaturation, calculated from the area under heat capacity peak, and the van't Hoff enthalpy, estimated from sharpness of the heat absorption peak, obtained under different solvent conditions, are listed in Table 1. In low salt, the ratio $\Delta H_{cal}/\Delta H_{vH}$ is lower than what is expected for a completely two-state transition, although agreement becomes quite good in the presence of 400 mM NaCl. This might be the result of incomplete reversibility of unfolding in solutions with low salt. Upon rescanning, it was found that reversibility increases with increasing NaCl concentration. In 200 mM NaCl, comparison of the shapes of the curves from the original and repeat scans indicates that denaturation is approximately 60% reversible. In the presence of 400 mM NaCl, analysis shows the denaturation to be approximately 90% reversible. Sturtevant (1987) and Privalov and Potekhin (1986) have pointed out that standard deconvolution techniques may be applied to processes that are less than 100% reversible. They argue that irreversibility of protein unfolding is generally caused by various secondary processes, such as proline isomerization, aggregation, etc. (Klibanov, 1983), and that these processes proceed much more slowly than unfolding and so have little effect on the denaturation profile. There will generally be some sharpening of the observed heat absorption peak, but the total area will not be significantly changed. Thus, accurate calorimetric enthalpy values can be obtained from a standard thermodynamic analysis, though van't Hoff enthalpy values will be increased somewhat relative to those seen for a 100% reversible process. This explains the low $\Delta H_{cal}/\Delta H_{vH}$ ratio noted above.

At pH 6.3, barstar is closer to its isoelectric point (estimated to be approximately 5.3) than it is under any of the other conditions studied. Moving closer to the isoelectric point results in an increased tendency to aggregate, and such aggregation is responsible for the anomalous shape of this curve.

The slope of the plot of the denaturational enthalpy versus the temperature (T_d) of denaturation, $\partial\Delta H/\partial T$, is 5.6 kJ K^{-1} mol^{-1} (Fig. 4), which is very close to the value of the denaturational heat capacity increment obtained from the original calorimetric curves (Table 1). This indicates that ionization effects do not contribute significantly to the total denaturation enthalpy.

Discussion

The most noteworthy result of this study is the observation that the measured enthalpy and entropy changes accompanying the disruption of barstar's native structure are unusually low in value. They are significantly lower than those of other small globular proteins when compared at similar temperatures (Fig. 5). At $T \approx 75$ °C, the enthalpy of barstar unfolding was observed to be 2.37 ± 0.13 (kJ mol^{-1})/residue, less than half the value calculated for barnase at the same temperature (Griko et al., 1994). The thermal and chemical denaturation of barstar was recently studied by optical methods by Agashe and Udgaonkar (1995). They estimated the van't Hoff enthalpy of unfolding (which was somewhat larger than our calorimetrically measured enthalpy) and noted that the enthalpy of barstar denaturation was somewhat lower than for other small globular proteins. The experimentally measured enthalpy values for barstar obtained

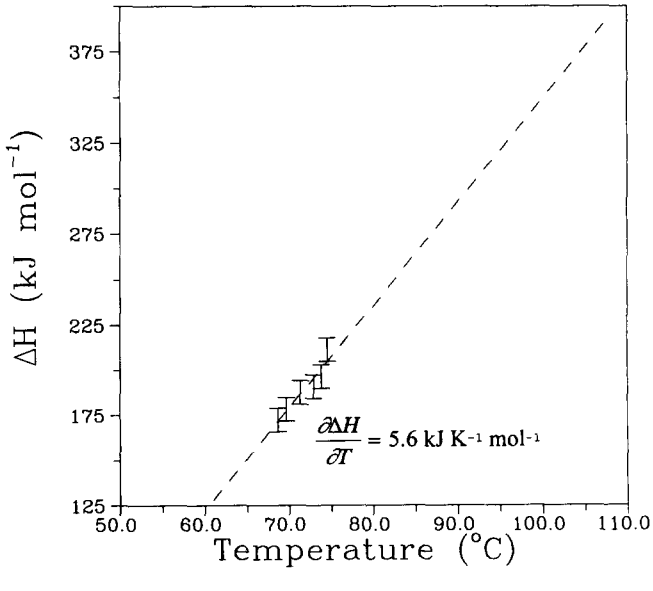

Fig. 4. Dependence of ΔH of barstar unfolding on temperature.

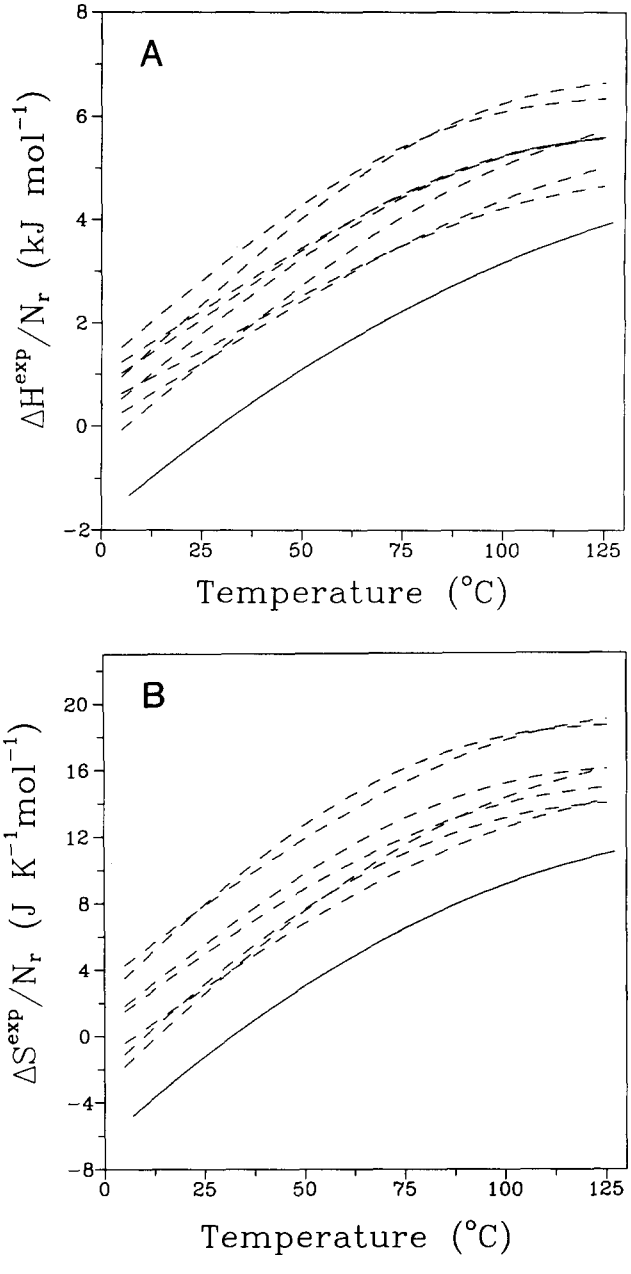

Fig. 5. The enthalpy (**A**) and entropy (**B**) change upon unfolding in units of kJ mol^{-1}/amino acid residue for barstar (solid line) and a number of other small globular proteins (dashed lines). Proteins are ROP protein, BPTI, chymotrypsin inhibitor 2, Eglin C, protein G, tendamistat, met-J repressor, and barnase. Data are taken from Makhatadze and Privalov (1995).

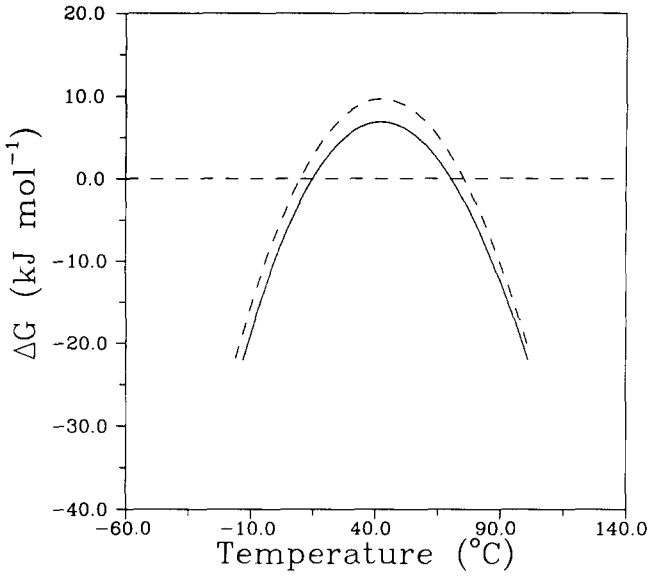

Fig. 6. Change in the Gibbs free energy upon barstar unfolding as a function of temperature. Solid line, pH 8.0; dashed line, pH 8.0, 400 mM NaCl.

in this study indicate an even more marked deviation from those of other proteins. Such low denaturational enthalpy values might indicate (1) that barstar does not unfold completely under the conditions of our experiments, in which case the enthalpy we observe is not the total enthalpy of unfolding but the enthalpy of transition to some partially unfolded state, or (2) the native structure of Cys 40, 82 Ala barstar is not as compact as that of typical globular proteins. Against the first of these suggestions are the facts that the posttransitional heat capacity was observed to be close to that calculated for the completely unfolded protein, and the far-UV CD spectra of barstar at 95 °C is very similar to that of barstar in 6 M GuHCl at 95 °C, where it is supposed exist as a random coil (Tanford, 1968).

Because the major contribution to the enthalpy of protein unfolding comes from the disruption of van der Waals interactions between amino acid groups packed in the native state (Makhatadze & Privalov, 1994), the low measured enthalpy of unfolding suggests that packing in native barstar is not as tight as in other proteins. This explanation is consistent with our observation that the partial specific heat capacity of native barstar is 0.37 ± 0.03 cal K^{-1} g^{-1}, slightly higher than what is observed for most globular proteins (0.30 ± 0.03 cal K^{-1} g^{-1}) (Privalov et al., 1989). Thus, according to both these experimental criteria, barstar has the characteristics of a protein with unusually flexible tertiary structure.

The low enthalpy and entropy of barstar denaturation lead to a restricted temperature range in which the native state is stable. Figure 6 shows the temperature dependence of ΔG for barstar unfolding at pH 8.0 in the presence of 0 and 400 mM NaCl. At pH 8.0, the native state is stable above ≈4 °C and below 70 °C, a range that is smaller than what has been observed for a number of other globular proteins (Privalov, 1979). The value of ΔG at 25 °C is estimated to be 4.1 ± 0.2 kcal mol^{-1}, which is in reasonable agreement with the value of 4.84 ± 0.18 kcal mol^{-1} estimated by Schreiber and Fersht (1993b).

In an attempt to clarify further the origins of the low enthalpy of barstar denaturation, we calculated the relative contributions of hydration and internal interactions to the observed thermodynamic parameters of barstar unfolding. The enthalpy and entropy of hydration upon protein unfolding can be estimated from changes in the water-accessible surface areas of aliphatic, aromatic, and polar groups going from the native to the unfolded state (Makhatadze & Privalov, 1993, 1995; Privalov &

Makhatadze, 1993). The enthalpy of hydration can be represented as

$$\Delta_N^U H^{hyd} = \Delta_N^U H_{pol}^{hyd} + \Delta_N^U H_{npl}^{hyd}$$

where

$$\Delta_N^U H_{pol}^{hyd} = \sum_i \Delta \hat{H}_i^{hyd} \Delta_N^U ASA_i,$$

i = polar part of amino acid side chain i, and

$$\Delta_N^U H_{npl}^{hyd} = \Delta \hat{H}_{arm}^{hyd} \Delta_N^U ASA_{arm} + \Delta \hat{H}_{alp}^{hyd} \Delta_N^U ASA_{alp}.$$

Likewise, the entropy of hydration can be represented as

$$\Delta_N^U S^{hyd} = \Delta_N^U S_{pol}^{hyd} + \Delta_N^U S_{npl}^{hyd}$$

where

$$\Delta_N^U S_{pol}^{hyd} = \sum_i \Delta S_i^{hyd} \Delta_N^U ASA_i,$$

i = polar part of amino acid side chain i, and

$$\Delta_N^U S_{npl}^{hyd} = \Delta S_{arm}^{hyd} \Delta_N^U ASA_{arm} + \Delta S_{alp}^{hyd} \Delta_N^U ASA_{alp}.$$

Figure 7A and B shows the enthalpy and entropy of hydration upon barstar unfolding as functions of temperature. Values are listed in Table 2. Also shown are the enthalpies and entropies of hydration of some typical small globular proteins: barnase, bovine pancreatic trypsin inhibitor (BPTI), hen egg white lysozyme, and ribonuclease A (Makhatadze & Privalov, 1994). From the figure it is clear that the enthalpy and entropy of hydration upon barstar unfolding are not significantly different from what is expected for comparable small globular proteins. Thus, it appears that the unusually low enthalpy and entropy of unfolding observed for barstar cannot be explained in terms of hydration effects.

The changes in enthalpy and entropy associated with the disruption of internal interactions in native barstar were calculated assuming (Makhatadze & Privalov, 1994):

$$\Delta_N^U H^{int} = \Delta_N^U H^{exp} - \Delta_N^U H^{hyd},$$

$$\Delta_N^U S^{int} = \Delta_N^U S^{exp} - \Delta_N^U S^{hyd}.$$

The values obtained are listed in Table 2. Figure 8A and B shows the enthalpy and entropy of internal interactions as functions of temperature. Also shown are the values obtained in previous studies for the same reference proteins listed above. It is clear that internal interactions in barstar are rather weak relative to many other small globular proteins, though they are not the weakest that have been measured (the weakest is BPTI). The results of these calculations support the conclusion that the unusually low denaturational enthalpy observed for barstar is due primarily to flexibility and weak internal interactions in the native state.

The interpretation of the low enthalpy of barstar denaturation as being due to weak internal interactions finds some support in recently published structural data. The structure of the barnase-barstar (Cys 40, 82 Ala) complex was recently determined by X-ray crystallography (Guillet et al., 1993; Buckle et al., 1994), and the solution structure of free wild-type barstar was solved by NMR spectroscopy (Lubienski et al., 1994). Lubienski et al. observed that the benzene ring of Phe-74 undergoes rapid ring flipping in the hydrophobic core of barstar, and have suggested that this might indicate a fluid or poorly packed hydrophobic interior. Interestingly, aromatic ring flipping in the hydrophobic interior has also been observed in BPTI (Richarz et al., 1980), which also seems to have unusually weak internal interactions. No structural changes were found between free barnase, and barnase complexed with barstar (Buckle et al., 1994), but significant differences were found between the structure of free barstar and barstar complexed with barnase. These differences have been characterized as rigid body outward movements of the four helices. Such an outward movement might involve disrupting favorable van der Waals contacts between the helices. However, if the interior of barstar is poorly packed to begin with, as our results suggest, then it will be able to rearrange its structure to optimize its contacts with barnase without disrupting energetically favorable, tightly packed internal interactions. Now that the energetics of barstar structure are known, this and other factors contributing to the stability of the barnase-barstar complex can be investigated in further calorimetric studies.

Table 2. *Total ΔH and ΔS of barstar unfolding*[a], *calculated contribution of hydration to the ΔH and ΔS of barstar unfolding, and contribution of internal interactions to ΔH and ΔS estimated by subtracting the contribution of hydration from the total*

	Temp. (K)					
	5	25	50	75	100	125
ΔH^{exp} (kJ mol^{-1})/N_r	−1.45 ± 0.1	−0.24 ± 0.1	1.10 ± 0.1	2.23 ± 0.1	3.16 ± 0.2	3.89 ± 0.2
ΔS^{exp} (kJ mol^{-1})/$N_r \cdot 10^3$	−5.33 ± 0.2	−1.24 ± 0.2	3.03 ± 0.2	6.48 ± 0.3	8.76 ± 0.4	10.94 ± 0.4
ΔH^{hyd} (kJ mol^{-1})/N_r	−44.92	−43.30	−41.21	−39.24	−37.34	−35.67
ΔS^{hyd} (kJ mol^{-1})/$N_r \cdot 10^3$	−59.85	−54.02	−47.29	−41.39	−34.41	−31.70
ΔH^{int} (kJ mol^{-1})/N_r	43.47 ± 0.1	43.06 ± 0.1	42.31 ± 0.1	41.47 ± 0.1	40.50 ± 0.2	39.56 ± 0.2
ΔS^{int} (kJ mol^{-1})/$N_r \cdot 10^3$	54.52 ± 0.2	52.78 ± 0.2	50.32 ± 0.2	47.87 ± 0.3	43.17 ± 0.4	42.64 ± 0.4

[a] Calculated from the experimentally measured ΔH and ΔS values and the temperature dependence of ΔC_p.
[b] N_r stands for the number of residues in the protein.

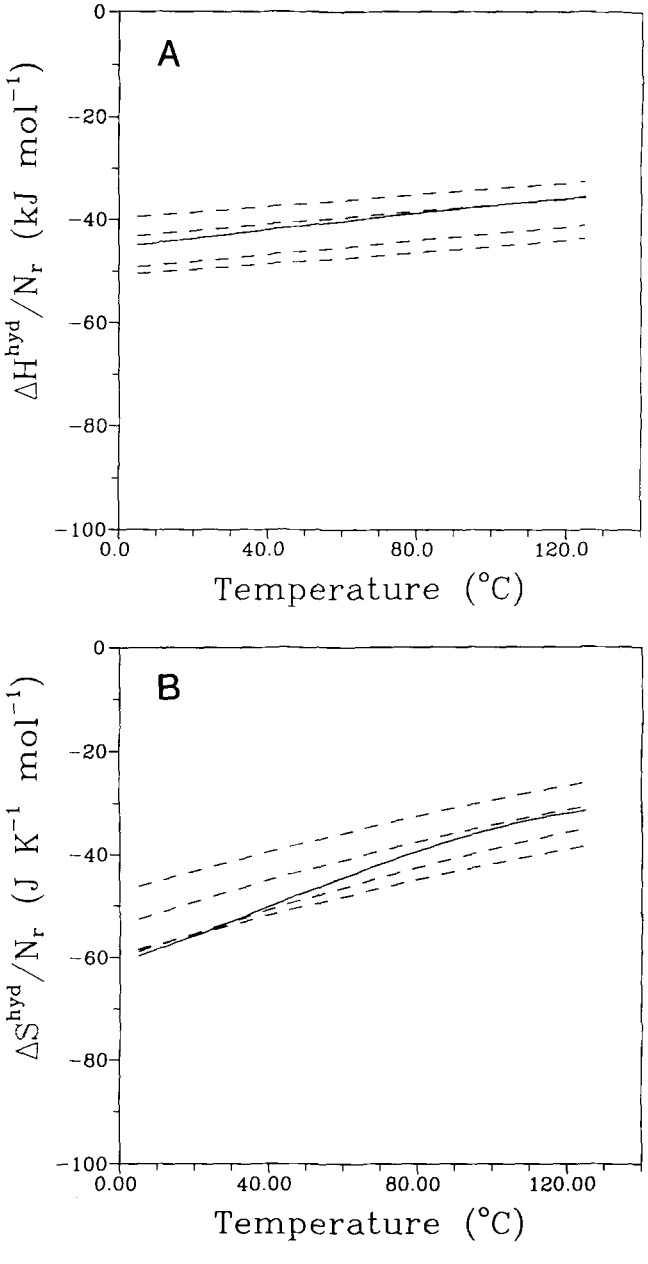

Fig. 7. The contribution of hydration to the change in enthalpy (**A**) and entropy (**B**) upon unfolding for barstar (solid line) and BPTI, bovine ribonuclease A, hen egg white lysozyme, and barnase (dashed lines). Data for reference proteins are from Makhatadze and Privalov (1994).

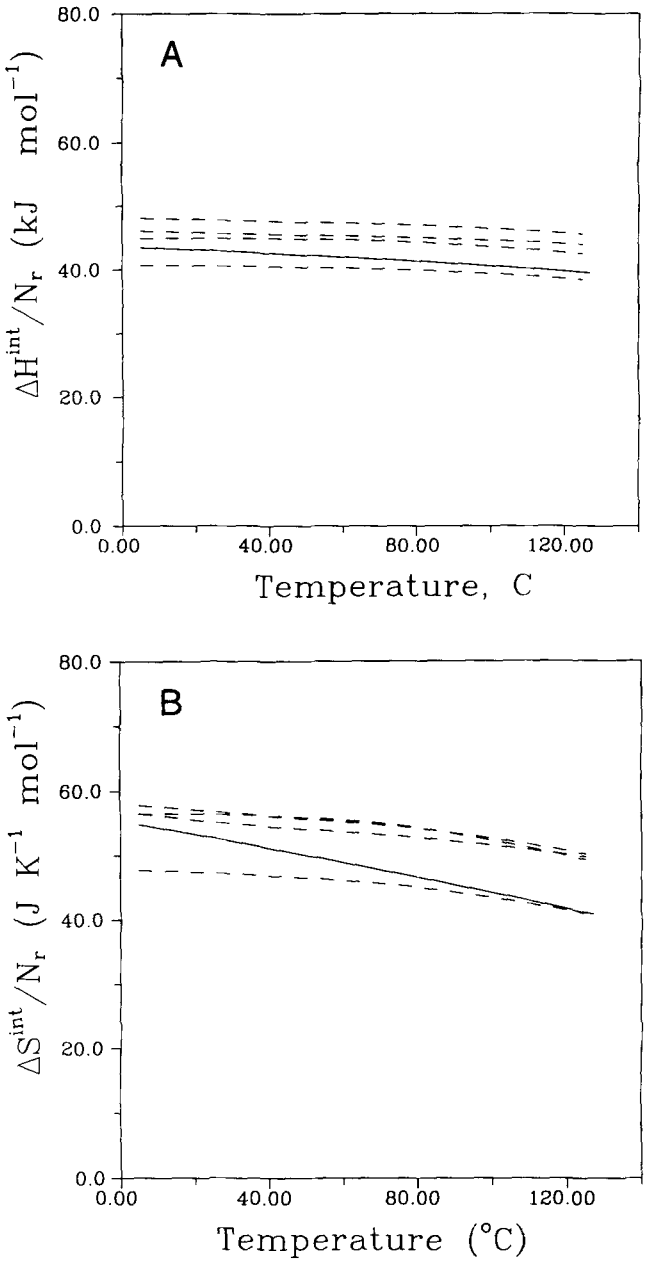

Fig. 8. The contribution of internal interactions to the change in enthalpy (**A**) and entropy (**B**) upon unfolding for barstar (solid line) and the same proteins in Figure 7 (dashed lines).

Materials and methods

The Cys 40, 82 Ala mutant of barstar was expressed in HB101 and purified using a modified version of the procedure used by Guillet et al. (1993). The purity of the final product was checked by SDS-PAGE stained with Coomassie blue. The concentration of barstar in solution was determined spectrophotometrically at 280 nm using the extinction coefficient $E^{1cm,1\%} = 19.4$ estimated by the method of Gill and von Hippel (1989). A correction for light scattering was made according to Winder and Gent (1971).

Calorimetric measurements were made using a calorimeter constructed at The Johns Hopkins University, at a heating rate of 1 deg/min. All protein solutions were dialyzed for 24–48 h against corresponding buffer solutions prior to scanning. Protein concentrations used varied from 0.9 to 1.6 mg/mL.

The partial specific heat capacity of the protein was determined according to Privalov and Potekhin (1986) assuming a molecular mass of 10,780 Da and a partial specific volume of 0.705 cm^3 g^{-1} at 25 °C, which was calculated from the amino acid sequence according to Makhatadze et al. (1990). The partial specific heat capacity of the unfolded protein was calculated

according to Privalov and Makhatadze (1990), using the known heat capacity values of amino acid residues (Makhatadze & Privalov, 1990) and assuming that, in the denatured protein, all amino acid residues are exposed to water and contribute additively to the heat capacity.

The surface areas of various groups of amino acid residues in barstar were calculated from its three-dimensional structure. Atomic coordinates (1bta) (Buckle et al., 1994) were obtained from the Brookhaven Protein Data Bank (Bernstein et al., 1977). The water-accessible surface areas of different groups in the native state were calculated using the program CAVT66 (Rashin, 1984) based on the algorithm developed by Shrake and Rupley (1973). The van der Waals radii used were the same as those of Chothia (1976), and the solvent probe radius was 1.4 $Å^2$. The water-accessible surface areas of groups in the unfolded state were calculated assuming the protein was a completely extended chain. The enthalpy and entropy of hydration were calculated from accessible surface area data according to Makhatadze and Privalov (1993) and Privalov and Makhatadze (1993).

CD spectroscopy was performed using a JASCO-700 spectropolarimeter. Measurements in the 250–190-nm range were made using a pathlength of 0.5 mm. Measurements in the 360–240-nm range were made using a pathlength of 0.5 cm. All protein solutions and buffers were passed through a 0.45-μm filter prior to measurement.

Thermodynamic analysis of the excess heat capacity functions obtained in the calorimetric experiments was performed according to Privalov and Potekhin (1986).

Acknowledgments

We are grateful to Dr. Robert W. Hartley for generously providing us with clones of Cys 40, 82 Ala barstar. We also thank Dr. George I. Makhatadze for his help in performing surface area calculations. This work was supported by National Institutes of Health grants GM 48036-01 and GM 48036, and National Science Foundation MCB 9118687.

References

Agashe VR, Udgaonkar JB. 1995. Thermodynamics of denaturation of barstar: Evidence for cold denaturation and evaluation of the interaction with guanidine hydrochloride. *Biochemistry 34*:3286–3299.

Bernstein FC, Koetzle TF, Williams GJB, Meyer EF Jr, Brice MD, Rodgers JR, Kennard O, Shimanouchi T, Tasumi M. 1977. The Protein Data Bank: A computer based archival file for macromolecular structures. *J Mol Biol 112*:535–542.

Buckle AM, Schreiber G, Fersht AR. 1994. Protein-protein recognition: Crystal structural analysis of a barnase-barstar complex at 2.0-Å resolution. *Biochemistry 33*:8878–8889.

Bycroft M, Ludvigsen S, Fersht AR. 1991. Determination of the three dimensional structure of barnase using nuclear magnetic resonance spectroscopy. *Biochemistry 30*:8697–8701.

Chothia C. 1976. The nature of the accessible and buried surfaces in proteins. *J Mol Biol 105*:1–14.

Gill SC, von Hippel PH. 1989. Calculation of protein extinction coefficients from amino acid sequence data. *Anal Biochem 182*:319–326.

Griko YV, Makhatadze GI, Privalov PL, Hartley RW. 1994. Thermodynamics of barnase unfolding. *Protein Sci 3*:669–676.

Guillet V, Lapthorn A, Hartley RW, Mauguen Y. 1993. Recognition between a bacterial ribonuclease, barnase, and its natural inhibitor, barstar. *Structure 1*:165–177.

Hartley RW. 1968. A reversible thermal transition of the extracellular ribonuclease of *Bacillis amyloliquefaciens*. *Biochemistry 7*:2401–2408.

Hartley RW. 1975. A two-state conformational transition of the extracellular ribonuclease of *Bacillis amyloliquefaciens* (barnase) induced by sodium dodecyl sulfate. *Biochemistry 14*:2367–2370.

Hartley RW. 1993. Directed mutagenesis and barnase-barstar recognition. *Biochemistry 32*:5978–5984.

Klibanov AM. 1983. Stabilization of enzymes against thermal denaturation. *Adv Appl Microbiol 29*:1–28.

Khurana R, Udgaonkar JB. 1994. Equilibrium unfolding studies of barstar: Evidence for an alternative conformation which resembles a molten globule. *Biochemistry 33*:106–115.

Lubienski MJ, Bycroft M, Freund SMV, Fersht AR. 1994. Three-dimensional solution structure and ^{13}C assignments of barstar using nuclear magnetic resonance spectroscopy. *Biochemistry 33*:8866–8877.

Makarov AA, Protasevich II, Kuznetsova NV, Fedorov BB, Korolev SV, Struminskaya NK, Bazhulina NP, Leshchinskaya IB, Hartley RW, Kirpichnikov MP, Yakovlev GI, Esipova NG. 1993. Comparative study of thermostability and structure of close homologues – Barnase and binase. *J Biomol Struct & Dyn 10*:1047–1065.

Makhatadze GI, Medvedkin VN, Privalov PL. 1990. Partial molar volumes of polypeptides and their constituent groups in aqueous solution over a broad temperature range. *Biopolymers 30*:1001–1010.

Makhatadze GI, Privalov PL. 1990. Heat capacity of proteins. I. Partial molar heat capacity of individual amino acid residues in aqueous solutions. Hydration effect. *J Mol Biol 213*:375–384.

Makhatadze GI, Privalov PL. 1993. Contribution of hydration to protein folding thermodynamics. I. The enthalpy of hydration. *J Mol Biol 232*: 1–21.

Makhatadze GI, Privalov PL. 1994. Hydration effects in protein unfolding. *Biophys Chem 51*:291–309.

Makhatadze GI, Privalov PL. 1995. Energetics of protein structure. *Adv Protein Chem 47*. Forthcoming.

Mauguen Y, Hartley RW, Dodson EJ, Dodson GG, Bricogne G, Chothia C, Jack A. 1982. Molecular structure of a new family of ribonucleases. *Nature 297*:162–164.

Privalov PL. 1979. Stability of proteins. *Adv Protein Chem 33*:167–237.

Privalov PL, Makhatadze GI. 1990. Heat capacity of proteins. II. Partial molar heat capacity of the unfolded polypeptide chain of proteins. *J Mol Biol 213*:385–391.

Privalov PL, Makhatadze GI. 1993. Contribution of hydration to protein folding thermodynamics. II. The entropy and Gibbs energy of hydration. *J Mol Biol 232*:660–679.

Privalov PL, Potekhin SA. 1986. Scanning microcalorimetry in studying temperature-induced changes in proteins. *Methods Enzymol 131*:4–51.

Privalov PL, Tiktopulo EI, Venyaminov SY, Griko YV, Makhatadze GI, Khechinashvili NN. 1989. Heat capacity and conformation of proteins in the denatured state. *J Mol Biol 205*:737–750.

Rashin A. 1984. Buried surface area, conformational entropy, and protein stability. *Biopolymers 23*:1605–1620.

Richarz R, Nagayama K, Wuthrich K. 1980. Carbon-13 nuclear magnetic resonance studies of internal mobility of the polypeptide chain in basic pancreatic trypsin inhibitor and a selectively reduced analogue. *Biochemistry 19*:5189–5196.

Sanz JM, Johnson CM, Fersht AR. 1994. The A state of barnase. *Biochemistry 33*:11189–11199.

Schreiber G, Fersht AR. 1993a. Interaction of barnase with its polypeptide inhibitor barstar studied by protein engineering. *Biochemistry 32*: 5145–5150.

Schreiber G, Fersht AR. 1993b. The refolding of *cis*- and *trans*-peptidylprolyl isomers of barstar. *Biochemistry 32*:11195–11203.

Shrake A, Rupley JA. 1973. Environment and exposure to solvent of protein atoms. Lysozyme and insulin. *J Mol Biol 79*:351–371.

Sturtevant J. 1987. Biochemical application of differential scanning calorimetry. *Annu Rev Phys Chem 38*:463–488.

Tanford C. 1968. Protein denaturation. *Adv Protein Chem 23*:121–282.

Winder AF, Gent WLC. 1971. Correction of light scattering errors on spectrophotometric protein determinations. *Biopolymers 10*:1243–1251.